Iranian Journal of Operations Research
Vol. 4, No. 2, 2013, pp. 127-145

Shape Optimization of an Arterial Bypass in Cardiovascular Systems

A.R. Nazemi[*,1], M.H. Farahi[2]

A high performance numerical technique in the study of aorto-coronaric bypass anastomoses configurations using steady Stokes equations is presented. The problem is first expressed as an optimal control problem. Then, by using an embedding method, the class of admissible shapes is replaced by a class of positive Borel measures. The optimization problem in measure space is then approximated by a linear programming problem. The optimal measure representing optimal shape is approximated by solving this finite-dimensional linear programming problem. An illustrative example demonstrates the effectiveness of the method.

Keywords: *Aorto-coronaric bypass anastomoses, Shape optimization, Optimal control, Stokes equation, Functional space, Linear programming.*

Manuscript was received on 19/12/2012, revised on 17/05/2013 and accepted for publication on 04/08/2013.

1. Introduction

When a coronary artery is affected by a stenosis, the heart muscle cannot be properly oxygenated through blood. Aorto-coronaric anastomosis restores the oxygen amount through a bypass surgery downstream an occlusion (see Figure 1). Improving the blood flow or hemodynamics in the synthetic bypass graft is an important element for the long-term success of bypass surgeries. It may also suggest new means in bypass surgical procedures as well as less invasive methods to devise new shape in bypass configuration [21].

In recent years, a number of algorithms for fast numerical solution of optimal shape design of an arterial bypass have been developed. For examples, Agoshkov et al. [3] applied optimal control by perturbation theory and provided a new approach to the problem, with the goal of improving arterial bypass graft on the basis of a better understanding of fluid dynamics aspects involved in the bypass study. Rozza [24] numerically investigated a reduced model based on Stokes equations and a vorticity cost functional (to be minimized) in the down-field zone of bypass based on an adjoint formulation. Quarteroni et al. [22] proposed a feedback procedure with Navier-Stokes fluid model based on the analysis of wall shear stress-related indexes. Zahab et al. in [6] discussed creation of a shape optimization suite consisting of a genetic algorithm, a meshless computational fluid dynamics solver, and an automated preprocessor. Finally, Abraham et al. in [1] and [2] presents some numerical studies of non-Newtonian effects on the solution of shape optimization problems involving steady and unsteady pulsatile blood flow, in an idealized two dimensional arterial graft geometry.

Figure 2 shows a picture of the human heart. Its functioning is very complex and various research teams are currently trying to develop satisfactory mathematical models of its mechanics, which involves, among other things, the study of electro-chemical activation of muscle cells. We will not cover this aspect here, but we concentrate on vascular flow and, in particular, flow in arteries. We

[*]Corresponding Author.
[1]Department of Applied Mathematics, School of Mathematical Sciences, Shahrood University of Technology, Shahrood, Iran, Email: nazemi20042003@yahoo.com.
[2]Department of Mathematical Sciences, Ferdowsi University of Mashhad, Mashhad, Iran, Email: farahi2001@yahoo.ie.

[Downloaded from iors.ir on 2024-04-25]

apply optimal control theory for shape optimization of aorto-coronaric bypass anastomoses based on an embedding method. We may encounter some aspects of this method in comparison with other numerical methods for optimal shape design problems. The method is not iterative, it is self-starting, and it is not restricted to differentiable cost functions. Due to these features, this approach has been successfully used to solve a variety of control, optimization and shape design problems (see [7]–[11], [13]–[20] and [25]).

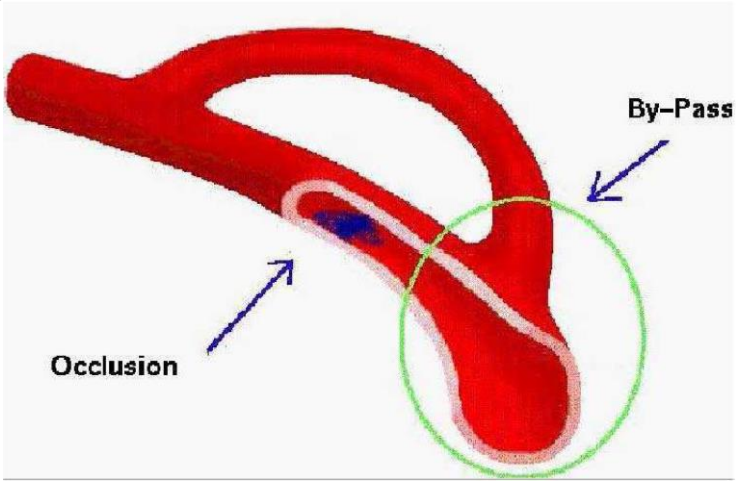

Figure 1: Simplified bypass model [22]

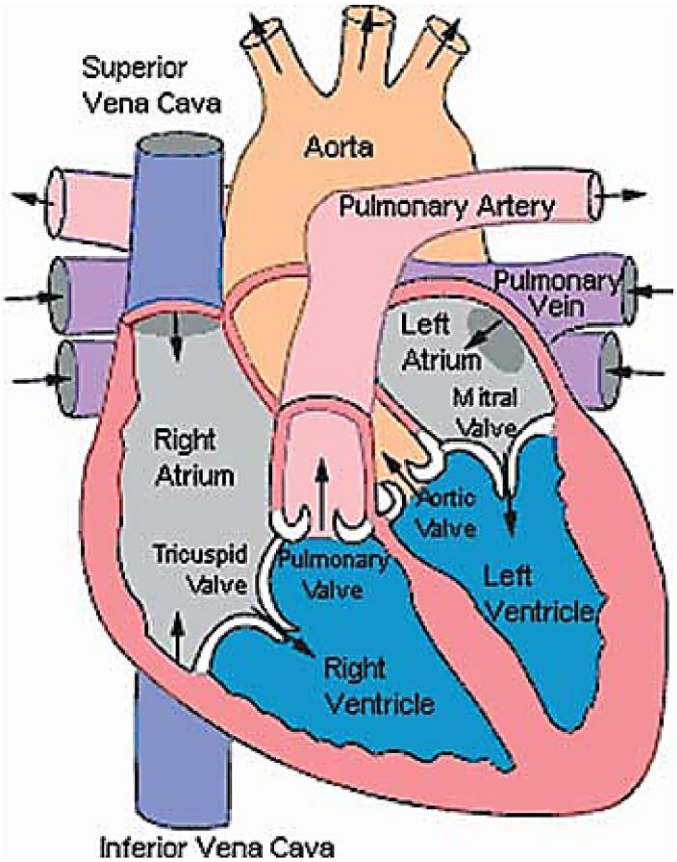

Figure 2. The human heart [23]

[Downloaded from iors.ir on 2024-04-25]

2. Mathematical Modelling of the Problem

Consider an idealized, two-dimensional bypass bridge configuration as in Figures 3, 4 and the domain on Figure 5, where the dotted line represents geometry of the complete anastomosis; Γ_{ω_2} is the section of the original artery, Γ_{in} is the new anastomosis inflow after bypass surgery, Γ_{out} is the anastomosis outflow.

We consider the following steady Stokes problem [3] in a domain $\Omega \subset \mathbb{R}^2$ with boundary Γ:

$$\begin{cases} -\nu\Delta\underline{v} + \nabla p = \underline{F} & in\ \Omega, \\ \nabla.\underline{v} = 0 & in\ \Omega, \\ \underline{v} = \underline{v}_{in} & on\ \Gamma_{in}, \\ \underline{v} = 0 & on\ f \cup \Gamma_{\omega_3}, \\ -p.n + \nu\dfrac{\partial \underline{v}}{\partial n} = \underline{g}_{out} & on\ \Gamma_{out} \cup \Gamma_{\omega_2}, \end{cases} \tag{1}$$

where $\underline{v} = (u, v)^T$ is the velocity, $n = (n_1, n_2)^T$ is the outward unit normal vector on Γ, $\underline{F} = \underline{F}(x, y)$ is a force field, $\underline{v}_{in} = \underline{v}_{in}(x, y)$, $\underline{g}_{out} = \underline{g}_{out}(x, y)$ are given vector functions, $\nu = const > 0$ is a kinematic viscosity, $\underline{v}_f = \{\underline{v}_{in}\ on\ \Gamma_{in};\ \underline{0}\ on\ f \cup \Gamma_{\omega_3}\}$, and f represents the sensible part of the bypass bridge determined.

The family of admissible sensible part f is characterized by

$$\mathcal{U}_{ad} = \{f \in C^{11}([0, a]);\ \beta_1 \le f(x) \le \beta_3, \text{ for all } x \in [0, a]\}, \tag{2}$$

where C^{11} denotes the space of functions whose first derivatives are Lipschitz continuous, and β_1 and β_3 are given constants.

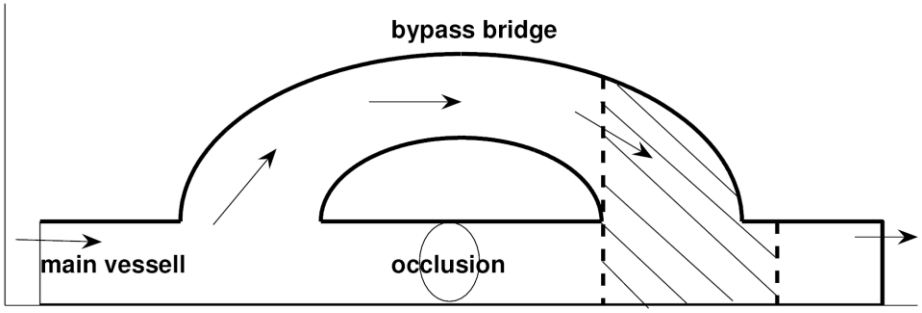

Figure 3. Idealized, 2-D bypass bridge configuration

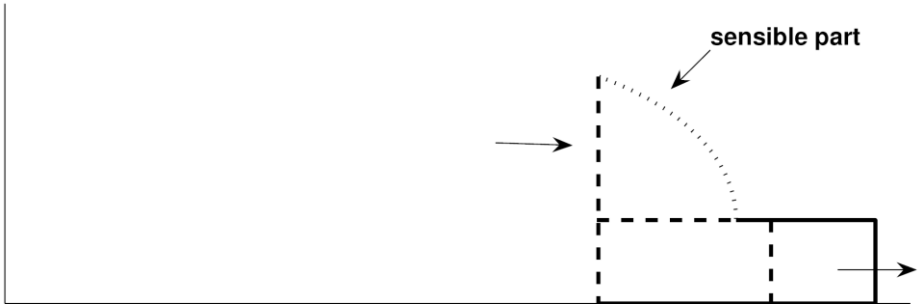

Figure 4. The dotted curve represents a possible shape variation

[Downloaded from iors.ir on 2024-04-25]

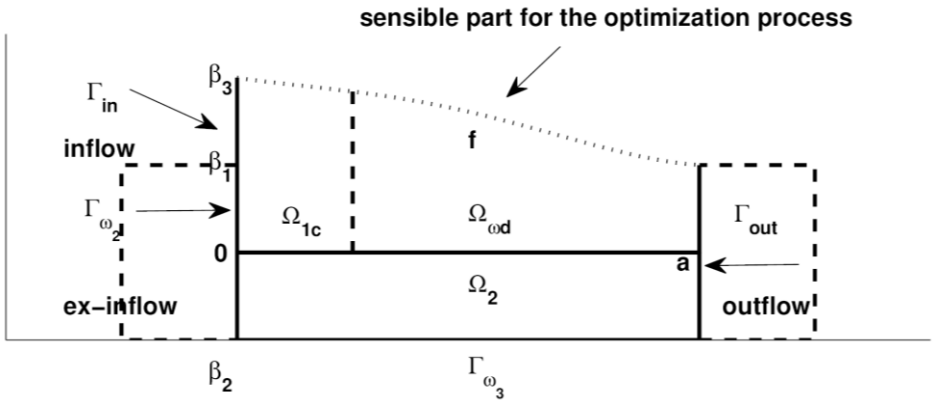

Figure 5. The dotted curve $\boldsymbol{f}$ represents the portion of the boundary that is subjected to change

The weak statement of (1) reads: find $\underline{v} \in (H^1(\Omega))^2$ and $p \in L^2(\Omega)$ such that

$$\begin{cases} a(\underline{v},\underline{\varphi}) = b(p,\underline{\varphi}) + g(\underline{\varphi}) & \forall \underline{\varphi} \in \mathcal{A}, \\ b(\psi,\underline{v}) = 0 & \forall \psi \in L^2(\Omega), \\ \underline{v} = \underline{v}_f & on\ \Gamma_{in} \cup f \cup \Gamma_{\omega_3}, \end{cases} \tag{3}$$

where with $\underline{\varphi}$ we indicate test functions, $\mathcal{A} = \{\underline{\varphi}: \underline{\varphi} \in (H^1(\Omega))^2, \underline{\varphi} = 0\ on\ \Gamma_{in} \cup f \cup \Gamma_{\omega_3}\}$ and

$$a\left(\underline{v},\underline{\varphi}\right) = \int_\Omega \nu\, \nabla \underline{v}.\nabla \underline{\varphi} dxdy,$$
$$b\left(p,\underline{\varphi}\right) = \int_\Omega p\, \nabla.\, \underline{\varphi} dxdy,$$
$$g(\underline{\varphi}) = \int_\Omega \underline{F}.\underline{\varphi} dxdy + \int_{\Gamma_{out}\cup\Gamma_{\omega_2}} \underline{g}_{out}.\underline{\varphi} d\Gamma.$$

3. Transformation onto Fixed Domain

In this section, we transform the problem (3) in weak variational form into a problem on a fixed domain. This is an efficient technique used in a variety of optimal shape design problems, for instance, see [16, 17, 18].

Let us consider domains $\Omega_1 = \{0 \le x \le a, 0 \le y \le f(x)\}$, $\Omega_2 = \{0 \le x \le a, \beta_2 \le y \le 0\}$, and $\Theta = \Theta_1 \cup \Theta_2$, as shown in Figure 6. Assume that $f(x) > 0$, and consider the following variable transformations:

[Downloaded from iors.ir on 2024-04-25]

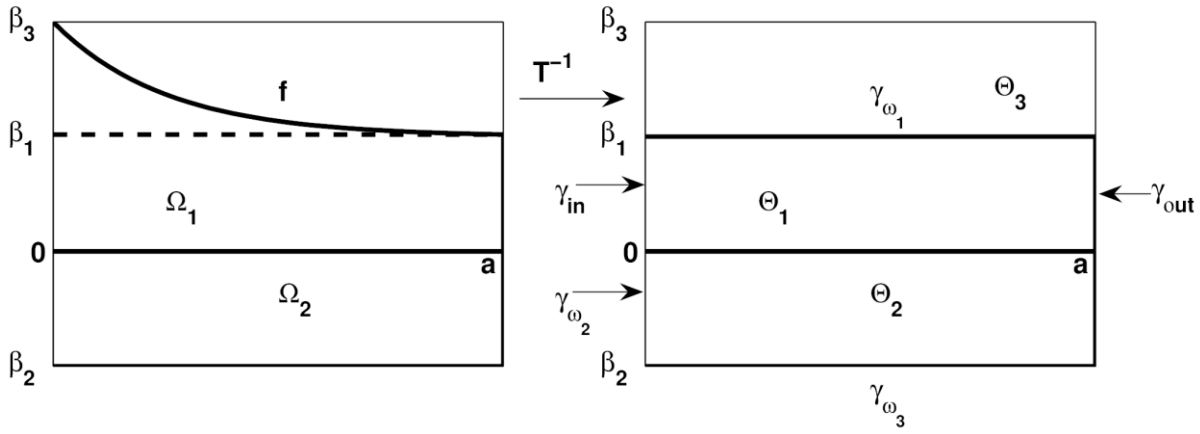

Figure 6. Transformation of the domain

$$T^{-1}: \Omega_1 \cup \Omega_2 \to \Theta,$$
$$T^{-1}(x,y)^T = (\tilde{x},\tilde{y})^T,$$

where T^{-1} is the identity in Ω_2, and $T^{-1}(x,y)^T = (x, \frac{\beta_1 y}{f(x)})^T$ in Ω_1.

The Jacobian of T, for all $(\tilde{x},\tilde{y}) \in \Theta_1$, is defined as:

$$J_T = \begin{pmatrix} 1 & 0 \\ \dfrac{\tilde{y} f'(\tilde{x})}{\beta_1} & \dfrac{f(\tilde{x})}{\beta_1} \end{pmatrix}, \quad \det J_T = \frac{f(\tilde{x})}{\beta_1} > 0.$$

Let $\underline{v}(x,y) = \underline{v}(T(\tilde{x},\tilde{y})) := \bar{\underline{v}}(\tilde{x},\tilde{y})$. Then $\nabla \underline{v}(x,y) = (J_{T^{-1}}^T)\nabla \bar{\underline{v}}(\tilde{x},\tilde{y})$, where

$$J_{T^{-1}} = \begin{bmatrix} \dfrac{\partial \tilde{x}}{\partial x} & \dfrac{\partial \tilde{x}}{\partial y} \\ \dfrac{\partial \tilde{y}}{\partial x} & \dfrac{\partial \tilde{y}}{\partial y} \end{bmatrix}.$$

The same relations exist for $\underline{v}(x,y), \underline{\varphi}(x,y), \psi(x,y), p(x,y), \underline{F}(x,y), \underline{g}_{out}(x,y)$, and $\underline{v}_{in}(x,y)$.

Using the chain rule, for each scalar function $\Phi(\tilde{x},\tilde{y})$, we have

$$\begin{cases} \dfrac{\partial \Phi}{\partial x} = \dfrac{\partial \Phi}{\partial \tilde{x}} - \beta y \dfrac{f'(x)}{f^2(x)} \dfrac{\partial \Phi}{\partial \tilde{y}}, \\ \dfrac{\partial \Phi}{\partial y} = \dfrac{\beta}{f(x)} \dfrac{\partial \Phi}{\partial \tilde{y}}. \end{cases} \tag{4}$$

To simplify the notations, from now on we will set (unless otherwise specified):

$$\tilde{x} = x, \tilde{y} = y, \bar{\underline{v}}(\tilde{x},\tilde{y}) = \underline{v}(x,y), \bar{\underline{\varphi}}(\tilde{x},\tilde{y}) = \underline{\varphi}(x,y), \bar{\psi}(\tilde{x},\tilde{y}) = \psi(x,y), \bar{p}(\tilde{x},\tilde{y}) = p(x,y),$$
$$\bar{\underline{F}}(\tilde{x},\tilde{y}) = \underline{F}(x,y), \bar{\underline{g}}_{out}(\tilde{x},\tilde{y}) = \underline{g}_{out}(x,y), \bar{\underline{v}}_{in}(\tilde{x},\tilde{y}) = \underline{v}_{in}(x,y).$$

[Downloaded from iors.ir on 2024-04-25]

Now, with the new variables, (3) is written as follows:

$$\begin{cases} a(f;\underline{v},\underline{\varphi}) - b(f;p,\underline{\varphi}) - g_1(f;\underline{\varphi}) = g_2(\underline{\varphi}) & \forall \underline{\varphi} \in \mathcal{B}, \\ b(f;\psi,\underline{v}) = 0 & \forall \psi \in L^2(\Theta), \\ c(f;\underline{v},\underline{v_f}) = 0, \end{cases} \tag{5}$$

where $\mathcal{B} = \{\underline{\varphi}: \underline{\varphi} \in (H^1(\Theta))^2 \text{ and } \underline{\varphi} = 0 \text{ on } \gamma_{in} \cup \gamma_{\omega_1} \cup \gamma_{\omega_3}\}$.

We have emphasized the dependence of $a(f;.,.), b(f;.,.)$, and $g(f;.)$ on f. Therefore,

$$a(f;\underline{v},\underline{\varphi}) = a_1(f;\underline{v},\underline{\varphi}) + a_2(\underline{v},\underline{\varphi}), \tag{6}$$

$$b(f;p,\underline{\varphi}) = b_1(f;p,\underline{\varphi}) + b_2(p,\underline{\varphi}), \tag{7}$$

$$g(f;\underline{\varphi}) = g_1(f;\underline{\varphi}) + g_2(\underline{\varphi}), \tag{8}$$

$$c(f;\underline{v},\underline{v_f}) = c_1(f;\underline{v},\underline{v_f}) + c_2(\underline{v},\underline{v_f}), \tag{9}$$

where

$$a_1\left(f;\underline{v},\underline{\varphi}\right) = \nu \int_{\Theta_1} \left((\nabla u)^T (J_{T^{-1}} J_{T^{-1}}^T)(\nabla \varphi_1) + (\nabla v)^T (J_{T^{-1}} J_{T^{-1}}^T)(\nabla \varphi_2)\right) \det J_T \, dxdy,$$

$$a_2\left(\underline{v},\underline{\varphi}\right) = \nu \int_{\Theta_2} ((\nabla u)^T (\nabla \varphi_1) + (\nabla v)^T (\nabla \varphi_2)) \, dxdy,$$

$$b_1\left(f;p,\underline{\varphi}\right) = \int_{\Theta_1} p \left(\frac{\partial \varphi_1}{\partial x} - \beta y \frac{f'(x)}{f^2(x)} \frac{\partial \varphi_1}{\partial y} + \frac{\beta}{f(x)} \frac{\partial \varphi_2}{\partial y}\right) \det J_T \, dxdy,$$

$$b_2(p,\underline{\varphi}) = \int_{\Theta_2} p \, (\frac{\partial \varphi_1}{\partial x} + \frac{\partial \varphi_2}{\partial y}) dxdy,$$

$$g_1\left(f;\underline{\varphi}\right) = \int_{\Theta_1} \underline{F} . \underline{\varphi} \det J_T \, dxdy,$$

$$g_2(\underline{\varphi}) = \int_{\Theta_2} \underline{F} . \underline{\varphi} dxdy + \int_{(\gamma_{out} \cup \gamma_{\omega_2}) \cap \partial\Theta_1} \underline{g_{out}} . \underline{\varphi} d\gamma + \int_{(\gamma_{out} \cup \gamma_{\omega_2}) \cap \partial\Theta_2} \underline{g_{out}} . \underline{\varphi} d\gamma,$$

$$c_1(f;\underline{v},\underline{v_f}) = \int_{\gamma_{in}} \| \underline{v} - \underline{v_f} \|_2^2 \, f(x) d\gamma + \int_{\gamma_{\omega_1}} \| \underline{v} - \underline{v_f} \|_2^2 \sqrt{1 + f'(x)^2} d\gamma = 0,$$

$$c_2(\underline{v},\underline{v_f}) = \int_{\gamma_{\omega_3}} \| \underline{v} - \underline{v_f} \|_2^2 \, d\gamma = 0.$$

4. Shape Optimization

It is assumed that $f(x)$ in (4) is unknown as well as $p, \underline{v}$. In order to determine the function $f(x)$, one can change the problem to an optimal control problem.

We consider the vorticity as distributed observation (flow control combined with shape

[Downloaded from iors.ir on 2024-04-25]

optimization) in the down-field zone $\Omega_{\omega d}$ of the incoming branch of the bypass, defined as $\nabla \times \underline{v} := rot(\underline{v}) = \frac{\partial v}{\partial x} - \frac{\partial u}{\partial y}$; $\underline{v}$ is the solution of the Stokes equations (1) and the control of the system (4) is obtained by minimizing the following cost functional:

$$\mathcal{J}(f) = \int_{\Omega_{\omega d}} (\nabla \times \underline{v})^2 dxdy, \tag{10}$$

where $\Omega_{\omega d} = \Omega_1 - \Omega_{1c}$ (see Figure 5).

Furthermore, the derivative of the unknown boundary $f(x)$ is chosen as a control function by the following dynamical system

$$\frac{df}{dx} = \mathcal{F}(\theta(x)), \tag{11}$$

with the boundary conditions

$$f(0) = \beta_3 \text{ and } f(a) = \beta_1, \tag{12}$$

where the trajectory function $f(x)$ is absolutely continuous, the control function $\theta(x)$ is Lebesgue-measurable, and $\mathcal{F}$ is a continuous function of $\theta(\cdot)$. Thus, the optimal shape design problem may be interpreted as an optimal control problem consisting of minimizing (10), subject to the constraints (11) and (12).

Definition 4.1. We say that the quadruple $\vartheta = (p, \theta, f, \underline{v})$ is admissible if following conditions hold:
(i) $\mathcal{F}(\theta(\cdot))$ satisfies (11).
(ii) $f(\cdot)$ is a decreasing differentiable function and satisfies (4), (11) and (12).
(iii) $(p, \underline{v})$ is a solution of (4).

We denote by $\mathcal{P}$ the set of all admissible quadruples. The control problem does not have a solution unless this set is nonempty.

Theorem 4.2. Each admissible shape of $\mathcal{U}_{ad}$ in (2) can be replaced exactly by one admissible quadruple $\vartheta = (p, \theta, f, \underline{v}) \in \mathcal{P}$.

Proof. It is enough to introduce an injection correspondence between $\mathcal{U}_{ad}$ and $\mathcal{P}$. For example,

$$\xi: \mathcal{U}_{ad} \to \mathcal{P},$$
$$\xi(f) = (p, \theta, f, \underline{v}).$$

By definition, ξ is one-to-one and onto. □

The above theorem enables us to consider the problem of minimizing $\mathcal{J}(\vartheta)$ over $\mathcal{P}$ instead of minimizing $\mathcal{J}(f)$ over $\mathcal{U}_{ad}$.

5. Optimization in Functional Space

In the following, the problem of shape optimization $\mathcal{J}(\vartheta)$ over $\mathcal{P}$ is transformed into another nonclassical problem which appears to have some better properties from computational point of view. Let $\Upsilon = D \times \mathcal{Q} \times \mathcal{U} \times \mathcal{C} \times \mathcal{K}$, where $D = (\Theta_1 \cup \Theta_2 \cup \Theta_3)$, $(\Theta_3 = [0, a] \times [\beta_1, \beta_3])$, $\mathcal{Q}$, $\mathcal{U}$ and $\mathcal{C}$ are known compact sets in R such that the pressure p, the optimal control $\theta(\cdot)$ and the unknown boundary $f(\cdot)$, respectively, get their values in these sets. Furthermore, $\mathcal{K}$ is a compact subset of

[Downloaded from iors.ir on 2024-04-25]

$R^2 \times R^2$, and $\nabla \underline{v}$ gets its values in this set.

For each admissible quadruple $\mathcal{P}$, we correspond a linear continuous functional Λ_ϑ as follows:

$$\Lambda_\vartheta : F \longrightarrow \int_D F\left(x, y, p(x), \theta(x), f(x), \nabla \underline{v}(x, y)\right) dxdy, F \in C(\Upsilon). \tag{13}$$

This linear function Λ_ϑ is defined on the space $C(\Upsilon)$ of all continuous real-valued functions F. Some aspects of this mapping are useful; it is well defined, linear, and positive.

Proposition 5.1. Transformation $\vartheta \to \Lambda_\vartheta$ of admissible quadruples in $\mathcal{P}$ into the linear mapping Λ_ϑ defined in (1) is an injection.

Proof. The proof is similar to proof for Proposition 4.1 of [10]. □

We need to convert (11) and (12) to integral form. For this purpose, let B be an open ball in $\mathbb{R}^2$ containing $[0, a] \times \mathcal{C}$, and $C^1(B)$ be the space of all real-valued continuous differentiable functions on it. Let $\phi \in C^1(B)$ and define functions ϕ^θ as follows:

$$\begin{aligned} \phi^\theta\big(x, y, p(x), \theta(x), f(x), \nabla \underline{v}\big) \\ = \phi_f\big(x, f(x)\big).\mathcal{F}\big(\theta(x)\big) + \phi_x\big(x, f(x)\big), \end{aligned} \tag{14}$$

for each $(x, y, p, \theta, f, \nabla \underline{v}) \in \Upsilon$. The function ϕ^θ is in the space $C(\Upsilon)$, the set of all continuous functions on the compact set . For each admissible quadruple $(p, \theta, f, \underline{v}) \in \mathcal{P}$, we have

$$\int_0^a \phi^\theta(x, y, p(x), \theta(x), f(x), \nabla \underline{v}) dx = \int_0^a \phi_f\left((x, f(x)).\mathcal{F}(\theta(x)) + \phi_x(x, f(x))\right) dx$$

$$= \int_0^a \frac{d}{dx}\{\phi(x, f(x))\} dx = \phi(a, f(a)) - \phi(0, f(0)) := \Delta_\phi, \tag{15}$$

for all $\phi \in C^1(B)$, where $\phi(a, f(a))$ and $\phi(0, f(0))$ are known. Define

$$\begin{aligned} H_\phi\big(x, y, p(x), \theta(x), f(x), \nabla \underline{v}\big): \\ = \frac{\phi^\theta\big(x, y, p(x), \theta(x), f(x), \nabla \underline{v}\big)}{\beta_3 - \beta_1}, \ \forall \phi \in C^1(B). \end{aligned} \tag{16}$$

From (15) and (16), we obtain

$$\int_{\beta_1}^{\beta_3} \int_0^a H_\phi\left(x, y, p(x), \theta(x), f(x), \nabla \underline{v}\right) dxdy = \Delta_\phi, \tag{17}$$

for each $\phi \in C^1(B)$.

Now, the integrand function in the objective functional (10) in terms of new variables changes

$$\begin{aligned} f_0\big(x, y, p(x), \theta(x), f(x), \nabla \underline{v}\big) = \chi_{\Omega_{\omega d}}\big(\nabla \times \underline{v}\big)^2 \det\left(J_T\right) = \\ \chi_{\Omega_{\omega d}}\left(\frac{\partial u}{\partial x} + \beta y \frac{f'(x)}{f^2(x)} \frac{\partial u}{\partial y} + \frac{\beta}{f(x)} \frac{\partial v}{\partial y}\right) \det J_T, \end{aligned}$$

where $\chi_{\Omega_{\omega d}}$ is the characteristic function on $\Omega_{\omega d}$ (see Figure 5). Thus, minimization of the

[Downloaded from iors.ir on 2024-04-25]

functional (10) over $\mathcal{P}$ is equivalent to finding Λ_ϑ in the functionals space $C^*(\Upsilon)$ (C^* is the dual space) that minimizes

$$\Lambda_\vartheta(f_0) \tag{18}$$

subject to

$$\Lambda_\vartheta(F_{\underline{\varphi}}) = \alpha_{\underline{\varphi}},\ \forall \underline{\varphi} \in \mathcal{B}, \tag{19}$$

$$\Lambda_\vartheta(I_\psi) = 0,\ \forall \psi \in L^2(\Theta), \tag{20}$$

$$\Lambda_\vartheta(G) = 0, \tag{21}$$

$$\Lambda_\vartheta(Z_\phi) = \Delta_\phi,\ \forall \phi \in C^1(B), \tag{22}$$

where

$$\begin{aligned} F_{\underline{\varphi}} \coloneqq\ & \chi_{\Theta_1}\nu\big((\nabla u)^T(J_{T^{-1}}J_{T^{-1}}^T)(\nabla\varphi_1) + (\nabla v)^T(J_{T^{-1}}J_{T^{-1}}^T)(\nabla\varphi_2)\big)\det J_T \\ & + \chi_{\Theta_2}\nu((\nabla u)^T(\nabla\varphi_1) + (\nabla v)^T(\nabla\varphi_2)) \\ & - \chi_{\Theta_1}p\left(\frac{\partial\varphi_1}{\partial x} - \beta y\frac{f'(x)}{f^2(x)}\frac{\partial\varphi_1}{\partial y} + \frac{\beta}{f(x)}\frac{\partial\varphi_2}{\partial y}\right)\det J_T - \chi_{\Theta_2}p\left(\frac{\partial\varphi_1}{\partial x} + \frac{\partial\varphi_2}{\partial y}\right) \\ & - \chi_{\Theta_1}\underline{F}.\underline{\varphi}\det J_T, \end{aligned}$$

$$\alpha_{\underline{\varphi}} \coloneqq g_2(\underline{\varphi}),$$

$$I_\psi \coloneqq \chi_{\Theta_1}\psi\left(\frac{\partial u}{\partial x} - \beta y\frac{f'(x)}{f^2(x)}\frac{\partial u}{\partial y} + \frac{\beta}{f(x)}\frac{\partial v}{\partial y}\right)\det J_T - \chi_{\Theta_2}\psi\left(\frac{\partial u}{\partial x} + \frac{\partial v}{\partial y}\right),$$

$$Z_\phi \coloneqq H_\phi\chi_{\Theta_3},$$

$$G \coloneqq \chi_{\gamma_{in}} \parallel \underline{v} - \underline{v_f} \parallel_2^2 f(x) + \chi_{\gamma_{\omega_1}} \parallel \underline{v} - \underline{v_f} \parallel_2^2 \sqrt{1 + f'(x)^2}d\gamma + \chi_{\gamma_{\omega_3}} \parallel \underline{v} - \underline{v_f} \parallel_2^2,$$

$\chi_{\gamma_{in}}, \chi_{\gamma_{\omega_1}}, \chi_{\gamma_{\omega_3}}, \chi_{\Theta_1}, \chi_{\Theta_2}$ and χ_{Θ_3} are respectively characteristic functions on $\gamma_{in}, \gamma_{\omega_1}, \gamma_{\omega_3}, \Theta_1$, Θ_2 and Θ_3.

6. Measure Theoretical Formulation

Let $M^+(\Upsilon)$ denote the space of all positive Radon measures on Υ. By the Riesz representation theorem [27], there is a one-to-one correspondence between $\Lambda \in C^*(\Upsilon)$ and $\mu \in M^+(\Upsilon)$ such that

$$\mu(F) = \int_\Upsilon F\, d_\mu,\ \forall F \in C(\Upsilon). \tag{23}$$

So, one may change the problem (18)–(22) in functional space to the following optimization problem in measure space:

$$\text{Minimize } \mu(f_0) \tag{24}$$

subject to

$$\mu(F_{\underline{\varphi}}) = \alpha_{\underline{\varphi}},\ \forall \underline{\varphi} \in \mathcal{B}, \tag{25}$$

$$\mu(I_\psi) = 0,\ \forall \psi \in L^2(\Theta), \tag{26}$$

$$\mu(G) = 0, \tag{27}$$

$$\mu(Z_\phi) = \Delta_\phi,\ \forall \phi \in C^1(B), \tag{28}$$

$$\mu \in M^+(\Upsilon). \tag{29}$$

Define the set of all positive Radon measures satisfying (25)-(29) as Q, and *topologize* the space $M^+(\Upsilon)$ by the weak*-topology. Consider the functional $\mathcal{J}: Q \longrightarrow \mathbb{R}$ defined by

[Downloaded from iors.ir on 2024-04-25]

$$\mathcal{J}(\mu) = \mu(f_0). \tag{30}$$

Now, the measure theoretical problem (24)–(29) may be interpreted as the problem of minimizing $\mathcal{J}$ over Q. Thus, it is necessary to verify the existence of a solution for this problem.

Theorem 6.1.
(i) The set Q consisting of all measures satisfying (25)–(29) is compact in $M^+(\Upsilon)$.
(ii) The functional $\mathcal{J}: Q \to \mathbb{R}$, defined by (30) is a linear continuous functional on the set Q with weak*-topology.
(iii) The measure-theoretic problem, which arises in finding the minimum of the functional $\mathcal{J}$ in (30) over the set Q of $M^+(\Upsilon)$, attains its minimum, say μ^*, in the set Q.

Proof. The proof is similar to Theorems 6.1 and 6.2 of [16]. □

Remark 6.2. Two main advantages for considering this measure theoretic form of the problem are:
(i) The existence of an optimal measure in the sets Q that satisfies (25)–(29) can be studied in a straightforward manner without needingg to impose conditions such as convexity which may be artificial.
(ii) The functionals in (24)–(29) are linear although the main problem may be nonlinear.

7. Approximation of the Optimal Measure

The minimizing problem (24)–(29) is an infinite-dimensional linear programming problem and we are mainly interested in approximating it. It is possible to approximate the solution of the problem (24)–(29) by the solution of a finite dimensional linear program of sufficiently large dimension.

First, we consider minimization of (24) not over the set Q but over a subset of it defined by requiring that only a finite number of constraints (25)–(29) be satisfied.

Consider the equalities of (25)–(29). Let the sets $\{\underline{\varphi_i}, i \in \mathbb{N}\}$, $\{\psi_j, j \in \mathbb{N}\}$ and $\{\phi_s, s \in \mathbb{N}\}$ be sets of total functions respectively in $\mathcal{B}$, $L^2(\Theta)$ and $\overline{C^1}(B)$. Now, we can prove the following proposition.

Proposition 7.1. Let $Q(M_1, M_2, M_3)$ be a subset of $M^+(\Upsilon)$ consisting of all measures satisfying

$$\mu(F_{\underline{\varphi_i}}) = \alpha_{\underline{\varphi_i}},\ i = 1,2,\dots,M_1, \tag{31}$$
$$\mu(I_{\psi_j}) = 0,\ j = 1,2,\dots,M_2, \tag{32}$$
$$\mu(G) = 0, \tag{33}$$
$$\mu(Z_{\phi_s}) = \Delta_{\phi_s},\ s = 1,2,\dots,M_3. \tag{34}$$

As M_1, M_2 and M_3 tend to infinity, $\varrho(M_1, M_2, M_3) = \inf_{Q(M_1,M_2,M_3)} \mu(f_0)$ tends to $\varrho = \inf_{Q} \mu(f_0)$.

Proof. The proof is similar to Proposition 2 of [11]. □

The first stage of the approximation is completed successfully. As the second stage, from Theorem $(A.5)$ of [26], we can characterize a measure, say μ^*, in the set $Q(M_1, M_2, M_3)$ at which the function $\mu \to \mu(f_0)$ attains its minimum. It follows from a result of Rosenbloom [28], as stated next.

Proposition 7.2. The measure μ^* in the set $Q(M_1, M_2, M_3)$ at which the function $\mu \to \mu(f_0)$ attains

[Downloaded from iors.ir on 2024-04-25]

its minimum has the following form

$$\mu^* = \sum_{k=1}^{M_1+M_2+M_3+1} \kappa_k^* \, \delta_{\Upsilon}(\iota_k^*), \tag{35}$$

where $\iota_k^* \in \Upsilon$ and $\kappa_k^* \geq 0,\ k = 1,2,\cdots, M_1 + M_2 + M_3 + 1.$

Here, $\delta_{\Upsilon}(\iota)$ is unitary atomic measures supported by singleton sets $\{\iota\}$, where $\iota \in \Upsilon$, and $\delta_{\Upsilon}(\iota_k^*)(F) = F(\iota_k^*)$, for all $F \in C(\Upsilon)$. Therefore, the measure theoretical optimization problem (24)–(29) is now equivalent to the following nonlinear optimization problem,

$$\text{Minimize} \sum_{k=1}^{M_1+M_2+M_3+1} \kappa_k^* \, f_0(\iota_k^*) \tag{36}$$

subject to

$$\sum_{k=1}^{M_1+M_2+M_3+1} \kappa_k^* \, F_{\underline{\varphi}_i}(\iota_k^*) = \alpha_{\underline{\varphi}_i}, i = 1,2,\dots, M_1, \tag{37}$$

$$\sum_{k=1}^{M_1+M_2+M_3+1} \kappa_k^* \, I_{\psi_i}(\iota_k^*) = 0, j = 1,2,\dots, M_2, \tag{38}$$

$$\sum_{k=1}^{M_1+M_2+M_3+1} \kappa_k^* \, G(\iota_k^*) = 0, \tag{39}$$

$$\sum_{k=1}^{M_1+M_2+M_3+1} \kappa_k^* \, Z_{\phi_s}(\iota_k^*) = \Delta\phi_s, s = 1,2,\dots, M_3, \tag{40}$$

$$\kappa_k^* \geq 0,\ k = 1,2,\dots, M_1 + M_2 + M_3 + 1, \tag{41}$$

where the unknowns are the coefficients κ_k^* and supports $\iota_k^*,\ k = 1,2,\dots, M_1 + M_2 + M_3 + 1.$
It would be computationally convenient if we could minimize the function $\mathcal{J}$ only with respect to the coefficients $\kappa_k^*,\ k = 1,2,\dots, M_1 + M_2 + M_3 + 1,$ which leads to a finite-dimensional linear programming problem. However, we do not know the supports of the optimal measures. The answer lies in approximation of this support, by introducing two dense subsets in Υ.

Proposition 7.3. Let σ be a countable dense subset of Υ. Given $\epsilon > 0$, a measures $\bar{\mu} \in M^+(\Upsilon)$ can be found such that

$$|(\mu^* - \bar{\mu})(f_0)| \leq \epsilon,$$
$$\left|(\mu^* - \bar{\mu})\left(F_{\underline{\varphi}_i}\right)\right| \leq \epsilon,\ i = 1,2,\dots, M_1,$$
$$\left|(\mu^* - \bar{\mu})\left(I_{\psi_j}\right)\right| \leq \epsilon,\ j = 1,2,\dots, M_2,$$
$$|(\mu^* - \bar{\mu})(G)| \leq \epsilon,$$
$$|(\mu^* - \bar{\mu})(Z_{\phi_s})| \leq \epsilon,\ s = 1,2,\dots, M_3.$$

where the measure $\bar{\mu}$ has the following form

[Downloaded from iors.ir on 2024-04-25]

$$\bar{\mu} = \sum_{k=1}^{M_1+M_2+M_3+1} \kappa_k^* \, \delta_{\Upsilon}(\iota_k), \tag{42}$$

and the coefficients κ_k^* are the same as the ones in the optimal measure (35) and $\iota_k \in \sigma$.

Proof. See the proof of Proposition III.3 in [26]. □

Thus, the nonlinear programming (36)–(41) can be approximated by the following linear programming problem

$$\text{Minimize} \quad \sum_{l=1}^{L} \kappa_l \, f_0(\iota_l) \tag{43}$$

subject to

$$\sum_{l=1}^{L} \kappa_l \, F_{\underline{\varphi}_i}(\iota_l) = \alpha_{\underline{\varphi}_i}, i = 1,2, \dots, M_1, \tag{44}$$

$$\sum_{l=1}^{L} \kappa_l \, I_{\psi_j}(\iota_l) = 0, j = 1,2, \dots, M_2, \tag{45}$$

$$\sum_{l=1}^{L} \kappa_l \, G(\iota_l) = 0, \tag{46}$$

$$\sum_{l=1}^{L} \kappa_l \, Z_{\phi_s}(\iota_l) = \Delta\phi_s, s = 1,2, \dots, M_3, \tag{47}$$

$$\kappa_l \geq 0, \; l = 1, \dots, L, \tag{48}$$

where ι_l, $l = 1,2, \dots, L$, belongs to σ and L is large enough. The procedure to construct a piecewise constant control function from the solution $\{\kappa_l\}$ of the linear programming problem (43)–(48), which approximates the action of the optimal measure, is based on the analysis presented in subsection 6.1 in [15].

8. Computer Simulation

To test our methodology, we consider a test problem on simplified configurations. Wall curvature was considered only in the zone of the incoming branch of the bypass $(0 \leq x \leq 4)$. Velocity values $\underline{v}_{in}$ at the inflow are chosen in such a way that the Reynolds number $Re = \frac{\bar{v}.D}{\nu}$ has order 10^3. The inlet Poiseuille velocity profile is chosen based on [4]:

$$\underline{v}_{in} = (-0.475(y-1)(y-2), -0.475(y-1)(y-2))^T.$$

Blood kinematic viscosity $\nu = \frac{\mu}{\rho}$ is equal to $4 \times 10^{-6} m^2 s^{-1}$, blood density is $\rho = 1 g c m^{-3}$ and dynamic viscosity is $\mu = 4 \times 10^{-2} g c m^{-1} s^{-1}$; $\bar{v}$ is mean inflow velocity related with $\underline{v}_{in}$, while D is the arterial diameter (3.5 mm); see [4] and [23].

[Downloaded from iors.ir on 2024-04-25]

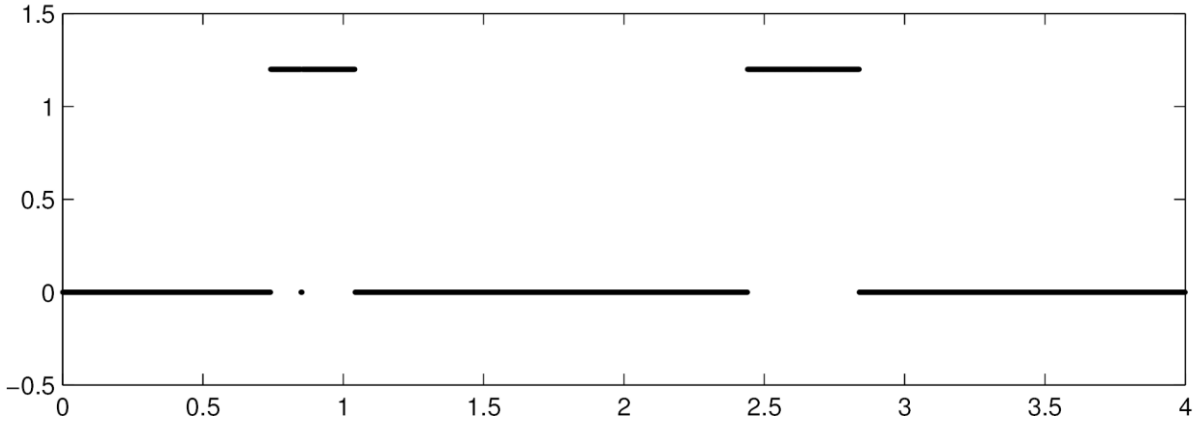

Figure 7. The approximate optimal artificial control

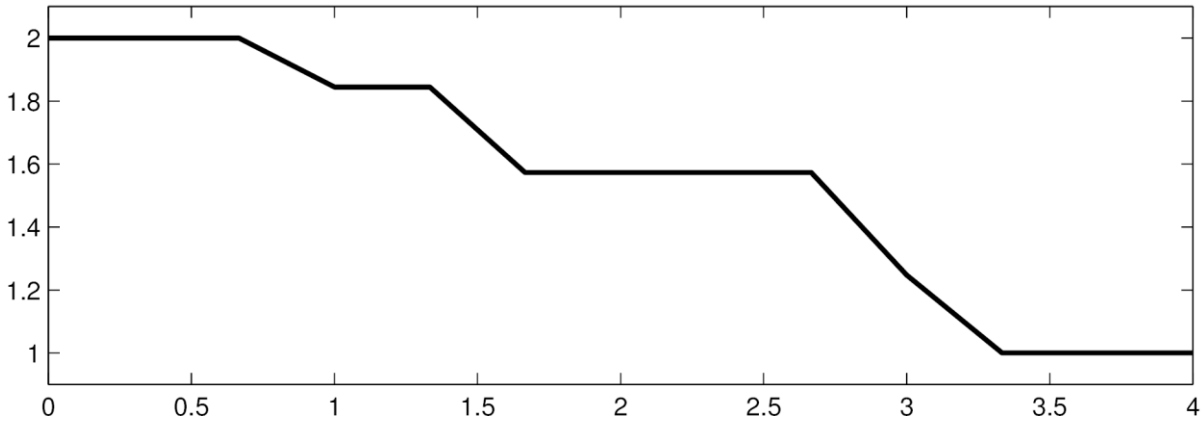

Figure 8. The exact optimal shape in the zone of the incoming branch of the bypass

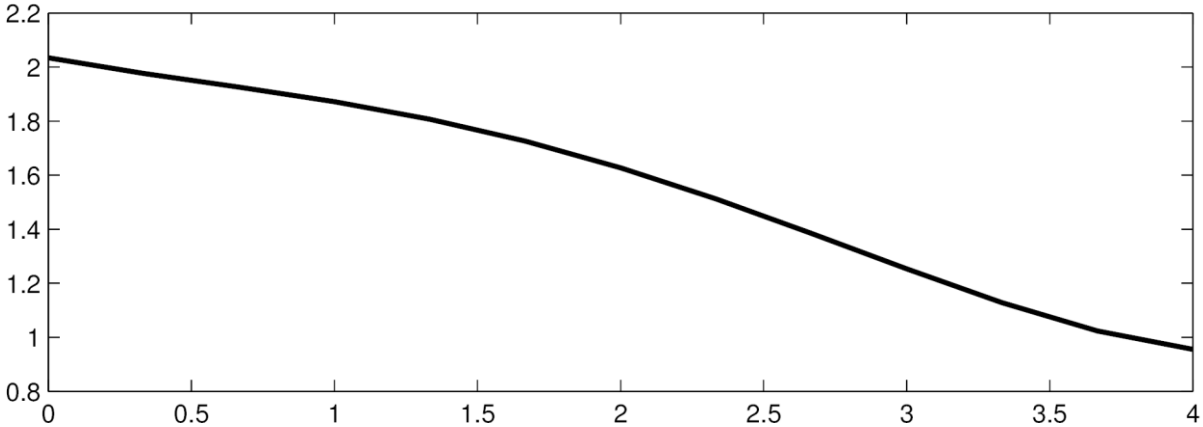

Figure 9. The approximate optimal shape of the bypass with fitting of degree 4

The geometric parameters are $a = 4$, $\beta_1 = 1$, $\beta_2 = -1$, and $\beta_3 = 2$. In objective function (10), we select $\Omega_{\omega d} = [0.5,4] \times [0, f]$, and in dynamical system (11) and (12), $\mathcal{F}(\theta) = -\theta^2(x)$. The functions in (1) are chosen as follows:

[Downloaded from iors.ir on 2024-04-25]

$$\underline{F}(x,y) = (xy, xy)^T, \ \underline{g}_{out}(x,y) = (xy, xy)^T.$$

For total functions of this example, we use M_1 test functions $\underline{\varphi} \in \mathcal{B}$ and M_2 test functions $\psi \in L^2(\Theta)$ of the forms

$$\underline{\varphi}(x,y) = (x^{a_1}(y-\beta_1)^{a_2}(y-\beta_2)^{a_3}, x^{b_1}(y-\beta_1)^{b_2}(y-\beta_2)^{b_3})^T.$$
$$\psi(x,y) = x^{c_1}y^{c_2},$$
$$a_1, a_2, a_3, b_1, b_2, b_3 \in \{1,2,\dots\}, \ c_1, c_2 \in \{0,1,2,\dots\}.$$

Moreover, we consider M_3 functions $\phi_s(x, f(x)) \in C^1(B)$ of three following types: Polynomials of the form:

$$x^{d_1} f^{d_2}, \ d_1, d_2 \in \{0,1,2,\dots\},$$

and functions with compact support as:

$$\sin\left(2k\pi(\frac{x}{a})\right), \ 1-\cos\left(2k\pi(\frac{x}{a})\right), \ (k = 1,2,\dots),$$

and finally, the piecewise constant functions as:

$$\theta_e = \begin{cases} 1, & \text{if } x \in J_e \\ 0, & \text{otherwise,} \end{cases}$$

where $J_e = (\frac{(e-1)a}{E}, \frac{ea}{E}), \ e = 1, \cdots, E$; for more details, see [10] and [11].

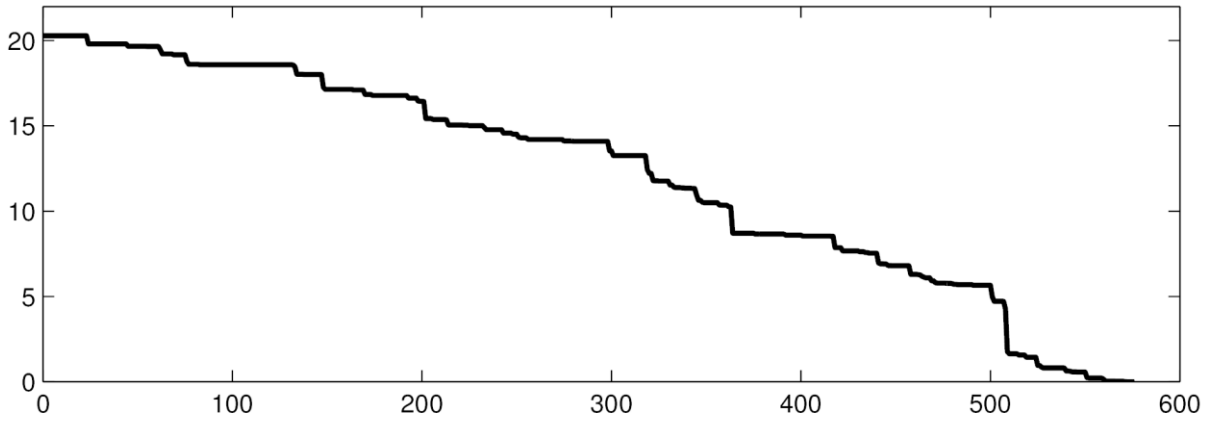

Figure 10. The transient behavior of the objective function over iterations

The set $\Upsilon = D \times \mathcal{Q} \times \mathcal{U} \times \mathcal{C} \times \mathcal{K}$ will be covered with a type grid, where the grid will be defined by taking all points in Υ as $\iota_l = (x_l, y_l, p_l, \theta_l, f_l, \nabla \underline{v}_l)$. The points in these grids will be numbered sequentially from 1 to L.

[Downloaded from iors.ir on 2024-04-25]

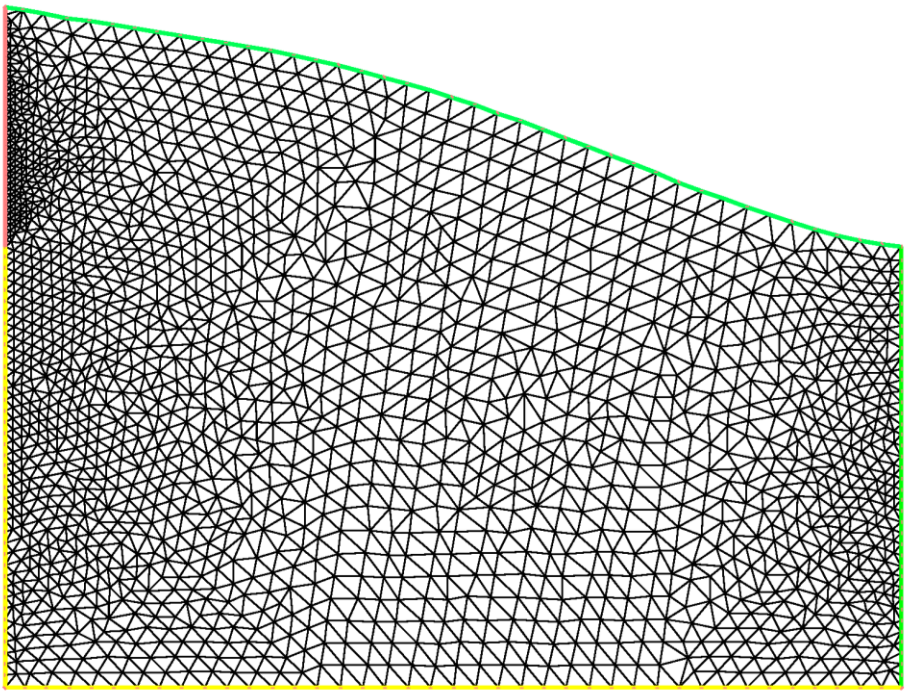

Figure 11. The adapted mesh of the domain $\boldsymbol{\Omega}$

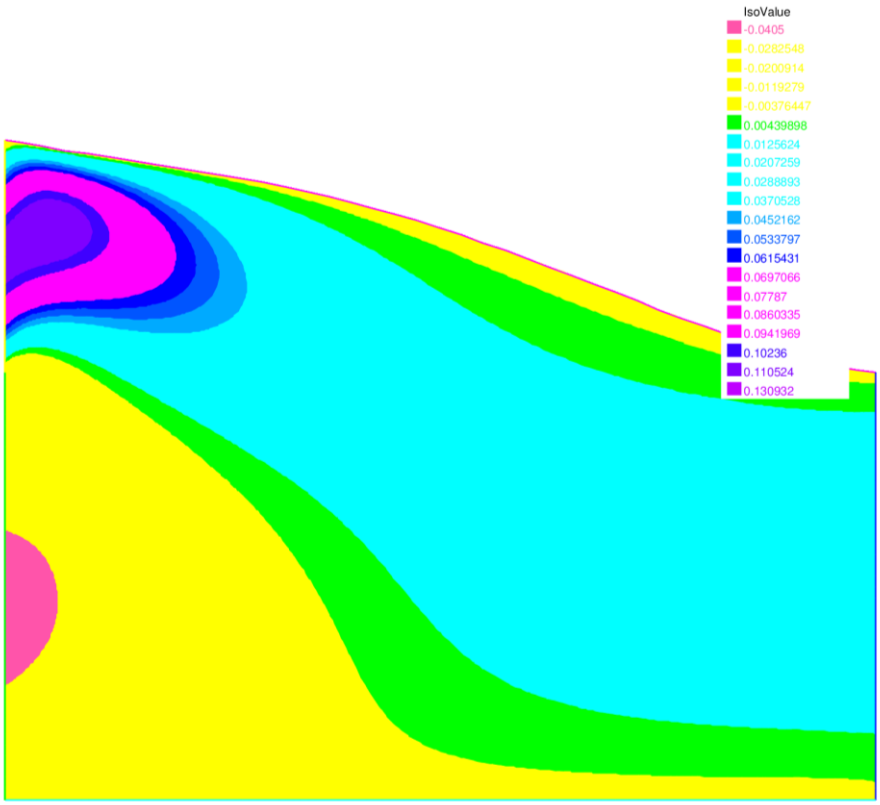

Figure 12. The contour of $\boldsymbol{u}(\boldsymbol{x}, \boldsymbol{y})$

[Downloaded from iors.ir on 2024-04-25]

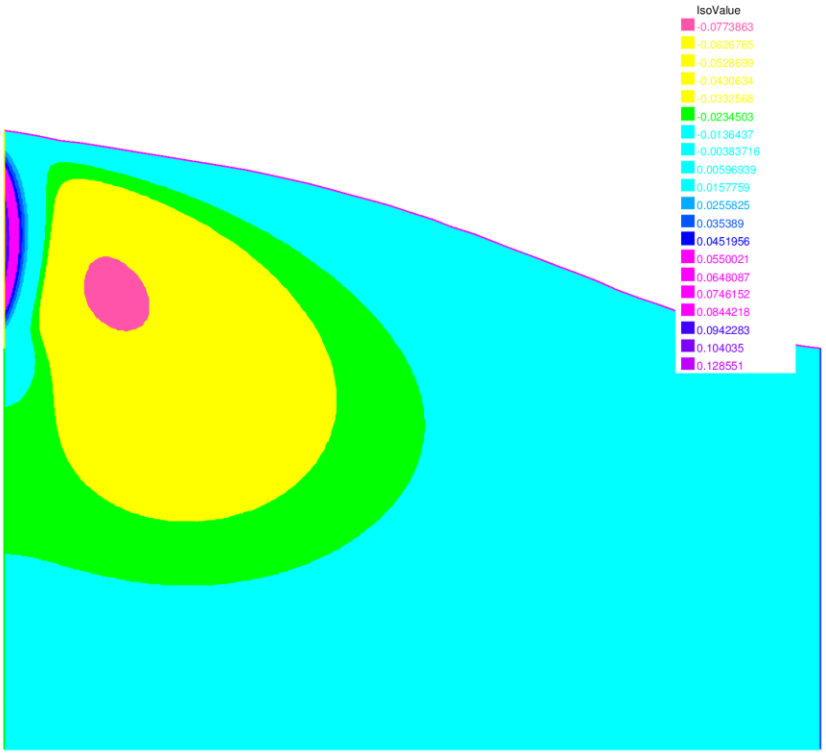

Figure 13. The contour of $\boldsymbol{v}(\boldsymbol{x},\boldsymbol{y})$

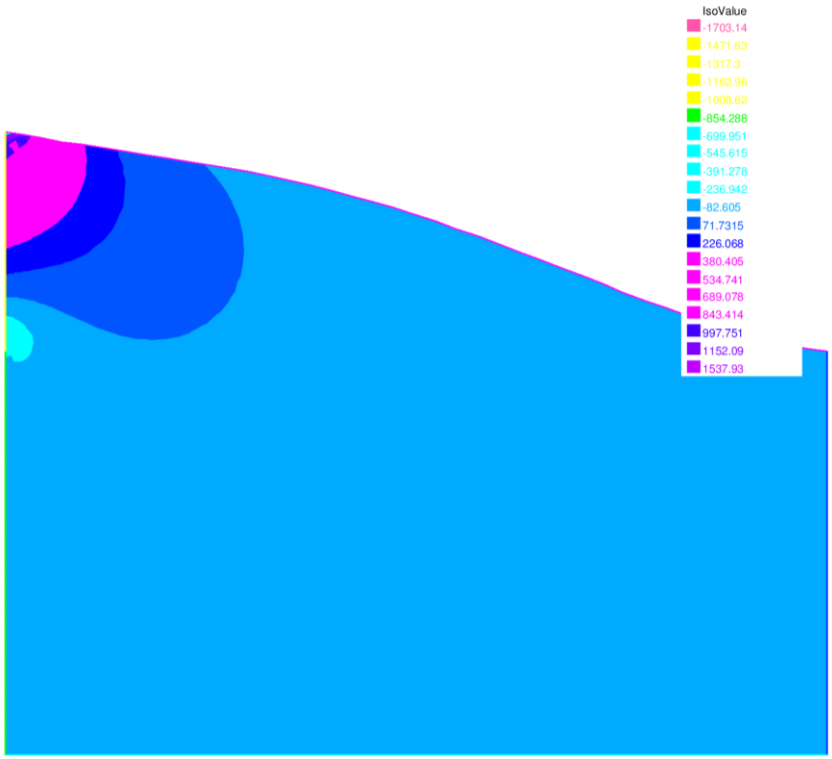

Figure 14. The contour of $\boldsymbol{p}(\boldsymbol{x},\boldsymbol{y})$

[Downloaded from iors.ir on 2024-04-25]

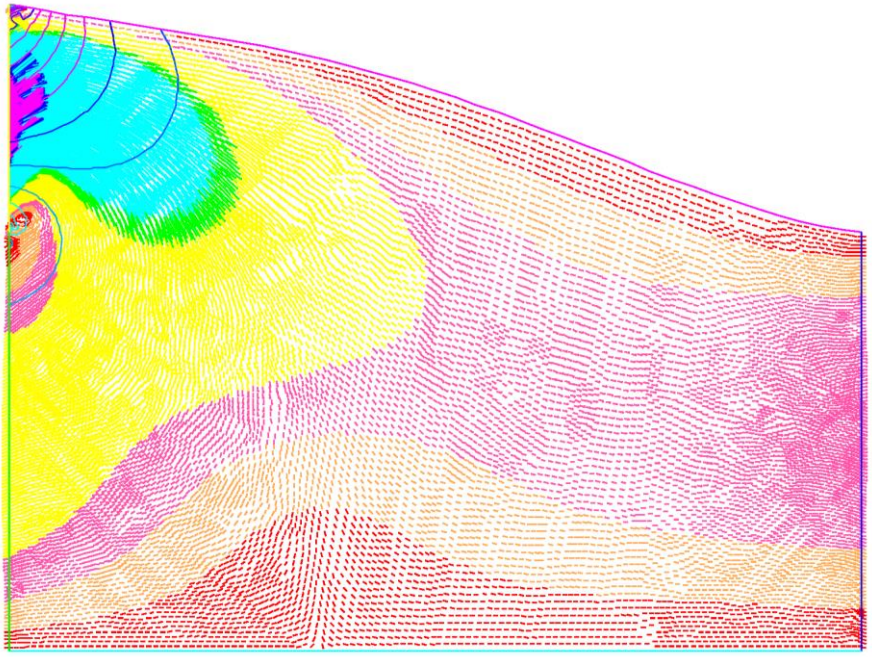

Figure 15. The vector field of the velocity and pressure $(\boldsymbol{u}, \boldsymbol{v}, \boldsymbol{p})^{\boldsymbol{T}}$

We solved the corresponding linear programming problem by means of a home-made revised simplex method [5] with $L = 3072$, $M_1 = 3$, $M_2 = 4$ and $M_3 = 9$. The optimal value of the cost function turned to be $\mathcal{J}^* = 4.7218 \times 10^{-8}$. We find the control function shown in Figure 7. This control function was used to design the optimal shape of bypass anastomoses in Figure 8. A numerical software was used to smooth the sensible part as shown in Figure 9 (see [29] for smoothing methods). Figure 10 illustrates decrease of the objective function over iterations for solving of the linear programming problem.

For this example, the approximate optimal shape of bypass, shown in Figure 9, is obtained as follows:

$$f(x) = 2.0342 - 0.1994x + 0.0973x^2 - 0.0706x^3 + 0.0105x^4.$$

By putting f in the weak form (3) of the stokes equation (1), and using FREEFEM++ software [12], the contours of u, v, p and the vector field of $(\underline{v}, p)^T$ are presented in Figures 11-15.

9. Conclusion

The theory of optimal control based on notations of the measure theory, functional analysis and linear programming was applied in order to optimize the shape of the zone of the incoming branch of the bypass (the toe) into the coronary. We fused the embedding procedure to convert the shape optimization problem to an optimal control problem. Then, to each admissible control-state, a linear continuous functional was associated. Correspondence between continuous positive linear functionals and positive Borel measures lead to an optimization problem in measure space. The transformed problem in measure space is an appropriate formulation of the optimal shape design problem since it is a linear programming problem in measure space. The solution of this linear programming problem was then approximated by the solution of a finite-dimensional linear program which is attractive for consistent numerical computations. The sub-optimal shape was found from the solution of the

[Downloaded from iors.ir on 2024-04-25]

corresponding linear programming. An interesting feature of this procedure is its straightforwardness. We estimate the optimal control and so the optimal shape directly, with no need for an initial solution.

Acknowledgments

The authors are grateful to the anonymous reviewer for his/ her suggestions in improving the presentation.

References

[1] Abraham, F., Behr, M. and Heinkenschloss, M. (2005), Shape optimization in steady blood flow: A numerical study of non-Newtonian effects, *Journal of Computer Methods in Biomechanics and Biomedical Engineering*, 8, 127-137.

[2] Abraham, F., Behr, M. and Heinkenschloss, M. (2005), Shape optimization in unsteady blood flow: A numerical study of non-Newtonian effects, *Journal of Computer Methods in Biomechanics and Biomedical Engineering*, 8, 201-212

[3] Agoshkov, V., Quarteroni, A. and Rozza, G. (2006), Shape design in aorto-coronaric bypass anastomoses using perturbation theory, SIAM, *Journal on Numerical Analysis*, 44, 367-384.

[4] Agoshkov, V., Quarteroni, A. and Rozza, G. (2006), A mathematical approach in the design of arterial bypass using unsteady stokes equations, *Journal of Scientific Computing*, 28, 139-165.

[5] Bazaraa, M.S., Jarvis, J.J. and Sherali, H.D. (1992), Linear Programming and Network Flows, John Wiley and Sons, New York.

[6] El Zahab, Z., Divo, E. and Kassaba, A. (2009), A meshless CFD approach for evolutionary shape optimization of bypass grafts anastomoses, *Journal of Inverse Problems in Science and Engineering*, 17, 411-435.

[7] Fakharzadeh, A. and Rubio, J.E. (1999), Shapes and measures, *IMA Journal of Mathematical Control & Information*, 16, 207-220.

[8] Fakharzadeh, A. and Rubio, J.E. (1999), Global solution of optimal shape design problems, *Zeitschrift für Analysis und ihre Anwendungen*, 18, 143-155.

[9] Farahi, M.H., Rubio, J.E. and Wilson, D.A. (1995), The optimal Control of the linear wave equation, *International Journal of Control*, 63, 833-848.

[10] Farahi, M.H., Mehne, H.H. and Borzabadi, A.H. (2006), Wing drag minimization by using measure theory, *Optimization Methods and Software*, 21 169-177.

[11] Farahi, M.H., Borzabadi, A.H., Mehne, H.H. and Kamyad, A.V. (2005), Measure theoretical approach for optimal shape design of a nozzle, *Journal of Applied Mathematics & Computing*, 17, 315-328.

[12] Hecht, F., Pironneau, O. and Ohtsuka, K. (2004), FreeFem++ Manual, http://www.freefem.org.

[13] Kamyad, A.V., Rubio, J.E. and Wilson, D.A. (1991), Optimal control of multidimensional diffusion equation, *Journal of Optimization Theory and Applications*, 70, 191-209.

[14] Kamyad, A.V., Rubio, J.E. and Wilson, D.A. (1992), Optimal control of multidimensional diffusion equation with a generalized control variable, *Journal of Optimization Theory and Applications*, 75, 101-132.

[Downloaded from iors.ir on 2024-04-25]

[15] Mehne, H.H. (2008), On solving constrained shape optimization problems for finding the optimum shape of a bar cross-section, *Journal of Applied Numerical Mathematics*, 58, 1129-1141.

[16] Mehne, H.H., Farahi, M.H. and Esfahani, J.A. (2005), On an optimal shape design problem to control a thermoelastic deformation under a prescribed thermal treatment, *Journal of Applied Mathematical Modelling*, 168, 1258-1272.

[17] Nazemi, A.R., Farahi, M.H. and Zamirian, M. (2008), Filtration problem in inhomogeneous dam by using embedding method, *Journal of Applied Mathematics and Computing*, 28, 313-332.

[18] Nazemi, A.R., Farahi, M.H. and Mehne, H.H. (2008), Optimal shape design of iron pole section of electromagnet, *Physics Letters A*, 372, 3440-3451.

[19] Nazemi, A.R. and Effati, S. (2010), Time optimal control problem of the wave equation, *Journal of Advanced Modeling and Optimization*, 12, 363-382.

[20] Nazemi, A.R. and Farahi, M.H. (2009), Control of the fibre orientation distribution at the outlet of contraction, *Journal of Acta Applicandae Mathematica*, 106, 279-292.

[21] Perktold, K., Hofer, M., Karner, G., Trubel, W. and Schima, H. (1998), Computer simulation of vascular fluid dynamics and mass transport: optimal design of arterial bypass anastomoses, in Proceedings of ECCOMAS, Papailion K et al. (eds.). Wiley, New York, 484-489.

[22] Quarteroni, A. and Rozza, G. (2003), Optimal control and shape optimization of aorto-coronaric bypass anastomoses, *Journal of Mathematical Models and Methods in Applied Sciences*, 13, 1801-1823.

[23] Quarteroni, A. and Formaggia, L. (2004), Mathematical modelling and numerical simulation of the cardiovascular system, in Modelling of Living Systems, Handbook of Numerical Analysis Series, P.G. Ciarlet and J.L. Lions, (eds.), North-Holland, Amsterdam.

[24] Rozza, G. (2005), On optimization, control and shape design of an arterial bypass, *International Journal of Numerical Methods in Fluids*, 47, 1411-1419.

[25] Rubio, J.E. (1995), The global control of nonlinear diffusion equations, *SIAM Journal on Control and Optimization*, 33, 308-322.

[26] Rubio, J.E. (1986), Control and Optimization: the Linear Treatment of Non-linear Problems, Manchester, U. K., Manchester University Press.

[27] Rudin, W. (1991), Functional Analysis, 2nd ed., McGraw-Hill, New York.

[28] Rosenbloom, P. C. (1952), Quelques classes de problems extremaux, *Bulletin de la Société Mathématique de France*, 80, 183-216.

[29] Stoer, J. and Bulirsch, R. (1992), Introduction to Numerical Analysis, Springer-Verlag, New York.

[Downloaded from iors.ir on 2024-04-25]